Accepted Manuscript

A moving boundary problem in a food material undergoing volume change – Simulation of bread baking

Emmanuel Purlis, Viviana O. Salvadori

PII: S0963-9969(10)00022-0
DOI: 10.1016/j.foodres.2010.01.004
Reference: FRIN 3103

To appear in: *Food Research International*

Received Date: 31 July 2009
Accepted Date: 19 January 2010

Please cite this article as: Purlis, E., Salvadori, V.O., A moving boundary problem in a food material undergoing volume change – Simulation of bread baking, *Food Research International* (2010), doi: 10.1016/j.foodres.2010.01.004

A moving boundary problem in a food material undergoing volume change – Simulation of bread baking

Emmanuel Purlis*, Viviana O. Salvadori

Centro de Investigación y Desarrollo en Criotecnología de Alimentos (CIDCA – CONICET La Plata), Facultad de Ciencias Exactas, UNLP, 47 y 116, La Plata (1900), Argentina

MODIAL, Facultad de Ingeniería, UNLP, 1 y 47, La Plata (1900), Argentina

Abstract

This paper presents a mathematical model for describing processes involving simultaneous heat and mass transfer with phase transition in foods undergoing volume change, i.e. shrinkage and/or expansion. We focused on processes where the phase transition occurs in a moving front, such as thawing, freezing, drying, frying and baking. The model is based on a moving boundary problem formulation with equivalent thermophysical properties. The transport problem is solved by using the finite element method and the Arbitrary Lagrangian-Eulerian method is used to describe the motion of the boundary. The formulation is assessed by simulating the bread baking process and comparing numerical results with experimental data. Simulated temperature and water content profiles are in good agreement with experimental data obtained from bread baking tests. The model well describes the stated general problem and it is expected to be useful for other food processes involving similar phenomena.

Keywords: Stefan problem; Moving mesh; Coupled transport; Expansion; Shrinkage; Thermophysical properties.

* Corresponding author. Phone/fax: +54 221 425 4853. E-mail: emmanuel@cidca.org.ar (E. Purlis)

1. Introduction

A large number of processes in food engineering involve simultaneous heat and mass transfer (SHMT) within the product. Coupled transport is due to changes in material properties with temperature and water content, as well as to gradients induced by transport phenomena, e.g. a temperature gradient can generate a water content gradient. In addition, the water contained in the food matrix can suffer phase change in several situations. For instance, thawing and freezing involve solid-liquid transition (fusion/solidification); drying (conventional, high temperature, spray-), frying and baking involve liquid-vapour transition (evaporation); freeze-drying and freezing (by surface dehydration) involve solid-vapour transition (sublimation). The phase transition takes place in a front which is actually a moving interface. Therefore, all these processes are catalogued as moving boundary problems – MBP (Farid, 2002).

On the other hand, changes in the volume of food, i.e. shrinkage and expansion, can occur during a process involving SHMT with phase transition. Shrinkage is a typical change observed during drying which happens due to loss of water and thermal stress in the cellular structure of foods (Mayor & Sereno, 2004), while expansion is a characteristic feature of the baking of leavened products (bread, cake). During baking, thermal expansion of carbon dioxide (produced by leavening agents) and water vapour present inside the porous structure deforms the dough increasing its volume until starch gelatinization occurs (Lostie, Peczalski, Andrieu & Laurent, 2002). Besides the texture and quality aspects related to volume change (Mayor & Sereno, 2004; Scanlon & Zghal, 2001), it is important from the mathematical modelling point of view to consider such phenomena since the variation in the system dimensions certainly modifies the temperature and water content gradients.

So far, few works have been published using the moving boundary analysis to model food processes regarding SMHT (Campañone, Salvadori & Mascheroni, 2001; Farid, 2002; Farid & Kizilel, 2009; Olguín, Salvadori, Mascheroni & Tarzia, 2008), but mostly not regarding the solution of a MBP coupled with volume change. This is probably due to difficulties associated with the numerical solution of this problem, the lack of understanding about shrinkage and expansion phenomena and their relationship with heat and mass transfer. The aim of this work was to develop a mathematical formulation for describing processes involving SHMT with phase transition in foods undergoing volume change. The formulation was focused on bread baking, but could be applied to any of the described situations previously. The proposed model was used to simulate the bread baking process under various experimental conditions, and the numerical results were compared with experimental data of temperature and water content.

2. Theory

Baking of bread is taken as the basis for developing a mathematical model for a process where a wet porous food undergoes SHMT with phase transition and volume change. Among the several complex changes occurring in bread during baking (Mondal & Datta, 2008), the main distinguishing features are the rapid heating of bread core and the development of a dry crust. The former has been explained by the evaporation-condensation mechanism (Bouddour, Auriault, Mhamdi-Alaoui & Bloch, 1998; de Vries, Sluimer & Bloksma, 1989; Sluimer & Krist-Spit, 1987; Wagner, Lucas, Le Ray & Trystram, 2007), while the later is due to the formation and advancing of an evaporation front towards the bread core (Zanoni, Peri & Pierucci, 1993; Zanoni, Pierucci & Peri, 1994). Certainly, bread baking can be classified as a drying-like process and therefore as a MBP. In this way, the bread can be modelled as a system containing three different regions: (1) crumb: wet inner zone, where temperature does not exceed 100 ºC and dehydration does not occur; (2) crust: dry outer zone, where temperature increases above 100 ºC and dehydration takes place; (3) evaporation front: between the crumb and crust, where temperature is ca. 100 ºC and water evaporates (liquid-vapour transition).

Furthermore, bread baking appears as a very particular case with respect to volume change. During the process, the dough firstly undergoes a volume increase due to thermal expansion of carbon dioxide and water vapour (until dough/crumb transition is reached), and then shrinkage due to the final crust formation and setting, where cross-linking reactions may occur (Sommier, Chiron, Colonna, Della Valle & Rouillé, 2005). An additional issue of this type of MBP is the vapour diffusion throughout the dried zone of the material, which is a more complicated situation than the classical MBP of melting or solidification (Farid, 2002). Therefore, bread baking appears as an adequate benchmark for modelling SHMT with phase transition in a wet porous food undergoing volume change.

Mathematically, a MBP (often called as Stefan problem) is related to time-dependent problems (i.e. parabolic type equations) where boundary position must be determined as a function of time and space (Crank, 1987). For instance, let us consider the melting of some material, in one dimension under boundary conditions of the first kind; this type of problem can be formulated considering the heat balance equation for each region, i.e. solid and liquid regions, with the corresponding initial and boundary conditions as follows:

Solid region:

$$C_1(T)\frac{\partial T}{\partial t} = \frac{\partial}{\partial x}\left(k_1(T)\frac{\partial T}{\partial x}\right), \quad 0 < x < S(t), \quad t > 0 \tag{1}$$

$$T_1(x,0) = \varphi_1(x) \leq T_f, \quad 0 < x < S(0) \tag{2}$$

$$T_1(0,t) = f_1(t) < T_f, \quad t > 0 \tag{3}$$

Liquid region:

$$C_2(T)\frac{\partial T}{\partial t} = \frac{\partial}{\partial x}\left(k_2(T)\frac{\partial T}{\partial x}\right), \quad S(t) < x < L, \quad t > 0 \tag{4}$$

$$T_2(x,0) = \varphi_2(x) \geq T_f, \quad S(0) < x < L \tag{5}$$

$$T_2(L,t) = f_2(t) > T_f, \quad t > 0 \tag{6}$$

On the interface between solid and liquid regions, where the phase change occurs, it is established that

$$T_1(S(t),t) = T_2(S(t),t) = T_f \tag{7}$$

$$k_2(T)\frac{\partial T_2}{\partial x} - k_1(T)\frac{\partial T_1}{\partial x} = \lambda\frac{\partial S}{\partial t} \tag{8}$$

This last boundary condition represents the *enthalpy jump* at the temperature of phase transition. Based on a physical approach, a different mathematical formulation is possible by defining an *equivalent* heat capacity per volume unit through the enthalpy definition (Bonacina, Comini, Fasano & Primicerio, 1973):

$$\widetilde{C}(T) = \frac{dH(T)}{dT} = C(T) + \lambda\delta(T - T_f), \quad C(T) = \begin{cases} C_1(T), & T < T_f \\ C_2(T), & T > T_f \end{cases} \tag{9}$$

where $\delta(T - T_f)$ is the delta function or "Dirac function", i.e. Eq. (9) implies that the phase change occurs at temperature T_f (Bracewell, 2000). Therefore, the two-region problem can be solved by only one partial differential equation with equivalent coefficients that include the phase change:

$$\widetilde{C}(T)\frac{\partial T}{\partial t} = \frac{\partial}{\partial x}\left(k(T)\frac{\partial T}{\partial x}\right), \quad k(T) = \begin{cases} k_1(T), & T < T_f \\ k_2(T), & T > T_f \end{cases} \tag{10}$$

For a generalized and unique solution to this problem, smoothed heat capacity and thermal conductivity must be defined in order to change within a temperature range rather than at a fixed temperature (Bonacina et al., 1973). Furthermore, the delta function in Eq. (9) is replaced by a delta-type function $\delta(T - T_f, \Delta T)$ so the phase change occurs in the semi-interval ΔT across T_f, where $\delta(T - T_f, \Delta T)$ is different from zero.

The formulation described above is used to solve one part of the problem; the other part is related to volume variation. As was previously stated, the expansion and shrinkage occurring in bread during baking involve several complex reactions and changes (Sommier et al., 2005). All these phenomena should be included in a comprehensive mathematical model for bread baking, which finally will result in a transport problem coupled with solid mechanics to describe the volume change. Although this is a general aim to achieve, the present article deals with the specific objective of developing a mathematical formulation for solving such complicated situation, i.e. a first (necessary) step. So, the volume change is included in an empirical way: the velocity of the boundary is prescribed and described through experimental data (see Sections 2.3 and 3 for details).

Finally, to develop the mathematical model for bread baking, the following major assumptions were used: (1) Bread is homogeneous and continuous; the porous medium concept is included through effective or apparent thermophysical properties. (2) Heat is transported by conduction inside bread according to Fourier's law, but an effective thermal conductivity is used to incorporate the evaporation-condensation mechanism in heat transfer. Note that we are aware of the increase in the water content of the bread core this phenomenon causes, but we assume this contribution to be negligible respect to the overall weight loss produced during baking (Purlis, 2007; Purlis & Salvadori, 2009a; Wagner et al., 2007). (3) Only liquid diffusion in the crumb and only vapour diffusion in the crust are assumed to occur (Luikov, 1975). (4) Water evaporates at 100 ºC (non-pressurized system).

2.1. Mathematical model for heat and mass transfer

We consider bread as an infinite cylinder of radius *R*, so a one dimensional problem can be obtained from the axial symmetry assumption. We suppose that the sample has uniform temperature and water content initially. Note that since bread undergoes volume change during baking the radius *R* is actually not constant.

2.1.1. Governing equations

Heat balance equation:

$$\rho C_p \frac{\partial T}{\partial t} = \frac{1}{r}\frac{\partial}{\partial r}\left(rk\frac{\partial T}{\partial r}\right) \tag{11}$$

Mass balance equation:

$$\frac{\partial W}{\partial t} = \frac{1}{r}\frac{\partial}{\partial r}\left(rD\frac{\partial W}{\partial r}\right) \tag{12}$$

2.1.2. Boundary conditions

The heat arriving to the bread surface by convection and radiation is balanced by conduction inside the bread:

$$-k\frac{\partial T}{\partial r}=h(T_s-T_\infty)+\varepsilon\sigma(T_s^4-T_\infty^4) \tag{13}$$

The water migrating towards the bread surface is balanced by convective flux:

$$-D\rho_s\frac{\partial W}{\partial r}=k_g\,(P_s(T_s)-P_\infty(T_\infty)) \tag{14}$$

where $P_s = a_w\, P_{sat}(T_s)$ and $P_\infty = (RH/100)\, P_{sat}(T_\infty)$.

At the centre, i.e. $r = 0$:

$$\frac{\partial T}{\partial r}=0 \tag{15}$$

$$\frac{\partial W}{\partial r}=0 \tag{16}$$

2.2. Thermophysical properties

In the MBP formulation, *equivalent* thermophysical properties are defined including the phase transition occurring during the process (water evaporation in bread baking), i.e. an equivalent property is valid for dough/crumb and crust. In this work, a smoothed Heaviside function with continuous derivative is used to incorporate the phase transition into thermophysical properties, according to previous description:

$$\delta(y,\Delta y)=((y_n>-1)\wedge(y_n<1))\times(0.5+y_n(0.75-0.25y_n^2))+(y_n\geq 1) \tag{17}$$

$$y_n=y/\Delta y \tag{18}$$

This (logical) expression approximates the step produced by phase change at T_f by smoothing the transition within the interval $-\Delta y < y < \Delta y$. In this work, $y = T - T_f$ and $\Delta y = \Delta T$, where $T_f = 100$ ºC and $\Delta T = 0.5$ ºC (Figure 1a). On the other hand, the delta-type function $\delta(T - T_f, \Delta T)$ describing the *enthalpy jump* is defined by the sum of two smoothed Heaviside functions with different sign (Figure 1a).

Following, the expressions and values for thermophysical properties of bread are briefly presented; for a detailed description, the reader is referred to Purlis (2007) and Purlis and Salvadori (2009b).

Specific heat (Figure 1b):

$$C_p(T,W) = C_p^*(T,W) + \lambda_v W \delta(T - T_f, \Delta T) \quad (19)$$

$$C_p^*(T,W) = C_{p,s}(T) + W C_{p,w}(T) \quad (20)$$

$$C_{p,s} = 5T + 25 \quad (21)$$

$$C_{p,w} = (5.207 - 73.17 \times 10^{-4} T + 1.35 \times 10^{-5} T^2)\, 1000 \quad (22)$$

Thermal conductivity (Figure 1b):

$$k(T) = \begin{cases} \dfrac{0.9}{1 + \exp(-0.1(T - 353.16))} + 0.2 & if \quad T \le T_f - \Delta T \\ 0.2 & if \quad T > T_f + \Delta T \end{cases} \quad (23)$$

Density:

$$\rho(T) = \begin{cases} 180.61 & if \quad T \le T_f - \Delta T \\ 321.31 & if \quad T > T_f + \Delta T \end{cases} \quad (24)$$

Density for solid (ρ_s) that appears in Eq. (14) is equal to 241.76 kg m^{-3}.

Mass diffusivity:

$$D(T) = \begin{cases} 1 \times 10^{-10} & if \quad T \le T_f - \Delta T \\ 1.32 \times 10^{-3} D_{va}(T) & if \quad T > T_f + \Delta T \end{cases} \quad (25)$$

Water activity:

$$a_w(T,W) = \left[\left(\frac{100\, W}{\exp(-0.0056T + 5.5)} \right)^{-1/0.38} + 1 \right]^{-1} \quad (26)$$

The heat transfer coefficient (h) is obtained from Nusselt number correlations, and the mass transfer coefficient (k_g) is determined by using the Chilton-Colburn (or heat-mass) analogy (Purlis & Salvadori, 2009b). Values for heat and mass transfer coefficients are summarized in Table 1. Respect to heat transfer by radiation, the emissivity of bread surface is considered equal to 0.9 (Hamdami, Monteau & Le Bail, 2004).

2.3. Volume change

The volume change is coupled to the transport model through a prescribed boundary velocity; we consider the sample radius to be a function of time, i.e. $R = R(t)$. To obtain the boundary velocity, an experimental procedure based on image processing was developed (see Section 4.2). So, the boundary velocity is calculated from the cross-section area values of bread at different times:

$$v_b = \frac{dR_{eq}}{dt} \cong \frac{R_{eq}^{n+1} - R_{eq}^{n}}{t^{n+1} - t^{n}} \tag{27}$$

with

$$R_{eq} = \sqrt{\frac{A}{\pi}} \tag{28}$$

Since bread samples are actually ellipsoidal rather than regular cylinders, we obtain an equivalent radius R_{eq} from the experimental data.

3. Numerical solution

The system of nonlinear partial differential equations describing the MBP stated in the previous section was solved using the finite element method (Zienkiewicz, 1989). The numerical procedure was implemented in COMSOL Multiphysics 3.2 (COMSOL AB, Sweden) and MATLAB 7.0 (The MathWorks Inc, USA). The Arbitrary Lagrangian-Eulerian (ALE) method was used to describe the motion of the boundary or volume change of food during the process. The ALE method is an intermediate approach between two classical descriptions of motion, the Lagrangian description and the Eulerian description, that combines the best features of these formulations. In the Lagrangian description each individual node of the mesh follows the associated material particle during motion, while in the Eulerian description the mesh is fixed and the continuum moves with respect to the grid. Lagrangian methods are mainly used in structural mechanics, where the displacements often are relatively small. On the other hand, Eulerian methods are widely used in fluid dynamics since large distortions in the continuum motion can be handled with relative ease, but generally at the expense of precise interface definition (Donea, Huerta, Ponthot & Rodríguez-Ferran, 2004). In the ALE description, the nodes of the computational mesh may be moved in some arbitrarily specified way to give a continuous rezoning capability, without the need for the mesh to follow the material movement. The main advantage of the ALE method is that there is no need for generating a new mesh at every time step; instead, the mesh nodes are perturbed, i.e. the mesh is deformed (Duarte, Gormaz & Natesan, 2004). The ALE method is popular in fluid dynamics and nonlinear solid mechanics but not in food engineering; only a few articles reported the use of this approach (Białobrzewski, 2006; Białobrzewski, Zielińska, Mujumdar & Markowski, 2008; Mascarenhas, Akay & Pikal, 1997).

In this work, the movement of the mesh was constrained only by a prescribed boundary condition, i.e. the system was subject to free displacement. In COMSOL Multiphysics, a Laplace smoothing method was applied to deform the mesh. In this way, the mesh displacement was obtained by solving a partial differential equation (the following explanation is valid for a general one-dimensional case):

$$\frac{\partial^2}{\partial X^2}\left(\frac{\partial x}{\partial t}\right) = 0 \tag{29}$$

This equation describes a coordinate transformation between two frames or coordinate systems (COMSOL AB, 2005):

- The spatial frame is the usual, fixed coordinate system with the spatial coordinate x. In this frame the mesh is moving, i.e. the coordinate x of a mesh node is a function of time.
- The reference frame is the coordinate system defined by the reference coordinate X. In this frame the mesh is fixed to its initial position. The reference frame can be seen as a curvilinear coordinate system that follows the mesh.

Therefore, $\frac{\partial x}{\partial t}$ represents the mesh velocity. In our model, the following boundary conditions can be established to solve Eq. (29):

$$\frac{\partial x}{\partial t} = 0, \qquad X = 0 \tag{30}$$

$$\frac{\partial x}{\partial t} = v_b(t), \quad X = L \tag{31}$$

So, the analytical solution for mesh velocity is:

$$\frac{\partial x}{\partial t} = v_b(t)\frac{X}{L} \tag{32}$$

This equation gives also the expression to relate spatial coordinate (x) with reference coordinate (X). For the present model, x represents r, while L is the initial radius of bread, R_0.

The solution procedure is summarized in Figure 2. The method of lines is used in COMSOL Multiphysics for discretization of the partial differential equation system describing the mathematical model (Eq. (11)-(26)), so a differential algebraic equation system is obtained (Fletcher, 1991). This new system is solved using an implicit time-stepping scheme (backward differentiation), i.e. a Newton's method together with a COMSOL Multiphysics linear system solver (UMFPACK). To incorporate the volume change, the solver assembles the discretized model on the deformed mesh using the ALE description. For this aim, the following expression is used:

$$\left.\frac{\partial u}{\partial t}\right|_x = \left.\frac{\partial u}{\partial t}\right|_X - \frac{\partial u}{\partial x}\frac{\partial x}{\partial t} \tag{33}$$

where u is a dependent variable. Eq. (33) is known as substantial or material derivative, and is used to relate the Lagrangian and Eulerian approaches (Welty, Wicks & Wilson, 1976). Then, Eq. (32) is used to compute Eq. (33), and the partial differential equations do not have to be reformulated.

For all simulations, the initial dimension of bread geometry was R_0 equal to 0.03 m, and the finite element mesh consisted in 240 elements. Relative humidity (or vapour pressure) in oven ambient was assumed to be negligible. A 30 min baking process was simulated for all conditions; the computing time was about 15 min using a PC with AMD Phenom™ 9550 Quad-Core Processor 2.20 GHz and 4 GB RAM. The time step taken by the algorithm is variable, but it was ensured to be small enough to do not miss the latent heat peak corresponding to phase transition.

4. Materials and methods

4.1. Bread samples

Samples were prepared using a standard recipe for French bread: wheat flour (100%), water (54.1%), salt (1.6%), sugar (1.6%), margarine (1.6%), and dry yeast (1.2%). Dough was made by mixing the ingredients for 10 min in a home multi-function food processor (Rowenta Universo 700 W, France) at constant speed. Then individual samples of 100-150 g (cylindrical shape, ca. 0.15 m length, 0.04 m diameter) were formed and placed in a perforated tray. After 1.5 h proving at ambient temperature, samples duplicated approximately their volume.

4.2. Baking tests

Dough samples were baked in an electrical static oven (Ariston FM87-FC, Italy) under two different baking conditions, depending on air velocity: natural convection (v = 0 m s^{-1}) and forced convection (v = 0.9 m s^{-1}). Experiments were carried out by duplicate using two oven temperatures: 200 and 220 ºC (±3.3 ºC). Temperature inside bread samples and in oven ambient was measured using T-type thermocouples (Omega, USA) connected to a data logger (Keithley DASTC, USA) which was incorporated to a PC; sampling time was set to 5 sec in all cases. The proving step was carried out inside the oven (turn off) to avoid any movement of thermocouples while introducing the tray inside the chamber. Thermocouples were placed in different positions of dough between the centre and the surface along the axial axis; final locations of thermocouples were determined after baking.

Water content was measured in five different regions along the vertical axis of the central cross-section (1 cm thickness) of bread samples (Figure 3). Water content for different baking times was determined by using different (but similar) samples, i.e. one sample for each time. Sampling was performed every 10 min for 200 ºC, and every 7 min for 220 ºC baking temperature. Also, moisture content of unbaked dough was determined. Water content values were calculated by drying the samples in a vacuum oven (Gallenkamp, United Kingdom) at 80 ºC, until constant weight was achieved. Crust thickness was determined using a calliper in the same experiments as water content. Four measures of each sample were recorded and then an average value was obtained for each baking time.

Volume change was determined by using a computer vision system through a similar protocol than for temperature measurement. At different baking times, images of the cross-section of a bread sample were acquired using a digital camera (Professional Series Network IP Camera Model 550710, Intellinet Active Networking, USA) and processed according to the following steps (Figure 4):

1. Conversion of original RGB image to grey-scale format.
2. Adjustment of image intensity values to increase the contrast.
3. Noise reduction by (linear) filtering to enhance image quality.
4. Segmentation through a global threshold value: a binary image is obtained where black colour (pixel value equal to 0) represents the background and white colour the sample (pixel value equal to 1).
5. Measurement of cross-section area.

Image processing was performed in MATLAB. Image acquisition was performed every 2 min for 200 ºC, while for 220 ºC, images were acquired every 1 min during the first 10 min of baking, and then every 2 min for the rest of the process. Additionally, to compare the influence of different patterns of volume change on heat and mass transfer by simulation, an extra condition was performed. Then, volume change was also measured (every 2 min) for 180 ºC baking under forced convection, which produces a continuous shrinkage of bread (Purlis, 2007). The obtained data was used to evaluate the boundary velocity of bread (Eq. (27)) during baking by linear interpolation. A detailed description of experimental procedures can be found in Purlis (2007) and Purlis and Salvadori (2009a).

5. Results and discussion

Representative temperature profiles obtained from baking tests and numerical simulation of the model are shown in Figures 5 and 6. Near the centre, temperature rises until reaches 100 °C asymptotically, showing a sigmoid trend; the rapid heating of the dough core has been explained through the evaporation-condensation mechanism (de Vries et al., 1989; Sluimer & Krist-Spit, 1987). On the other hand, surface temperature increases continuously up to 100 ºC, when water evaporation occurs, and then rises again towards the oven air temperature. At this location, the variation of temperature is almost linear, except for the plateau accounting for phase transition (Figure 6a). Finally, at the intermediate zone between the centre and the surface, the temperature increases showing hybrid behaviour: it does not surpass 100 °C as the core, but the variation before reaching the plateau is similar to the surface trend. As can be seen in Figures 5 and 6, the mathematical model predicts very well the variation of crumb temperature, and reproduces the experimental trend of crust in an acceptable way. The goodness of the model prediction was assessed by the mean absolute percentage error defined as (Heizer & Render, 2004):

$$e_{abs}(\%) = \frac{100}{n}\sum_{i=1}^{n}\left(\frac{\left|T_{experimental} - T_{predicted}\right|}{T_{experimental}}\right)_i \qquad (34)$$

where n is the number of temperature values taken into account. The calculated prediction errors corresponding to Figures 5 and 6 are summarized in Table 2.

Prediction errors for temperature at core and intermediate zones were between 1.16 and 3.18%, but were higher for the crust zone (though less than 10%).

Figure 7 presents typical variation of water content and crust thickness in bread during baking. Outer zones of bread suffer dehydration during all the process (Figure 7a), which actually leads to the formation and enlargement of a dry crust (Figure 7b). On the other hand, the moisture content at inner zones is almost the same as for unbaked dough, throughout baking. Furthermore, we could experimentally detect an increase between 0.4 and 2.3% respect to initial condition (in all experiments) that could not be reproduced by simulation since it is due to the evaporation-condensation mechanism, which was not included in the model. Regarding the prediction of surface moisture, the model presented differences between 0.01 (at 14 and 21 min for 220 ºC under natural convection, and 30 min for 200 ºC under forced convection) and 0.09 (at 20 min for 200 ºC under natural convection, and 7 min for 220 ºC under forced convection) kg kg^{-1} (dry basis) in comparison with experimental values (Table 3).

The simulated values of crust thickness were computed as the distance between the evaporation front and the bread surface. In this way, the position of phase transition front was defined as the point where water content gradient presented a minimum (Zhang & Datta, 2004). Simulation results show that the model overestimates crust thickness during baking (Figure 7b and Table 3); differences were between 0.5 (at 7 min for 220 ºC under natural convection) and 6 (at 21 and 28 min for 220 ºC under forced convection) mm, which increased with baking time, and heat and mass fluxes. This can be attributed to the definition of crust region used in each case, i.e. experiments and simulation. In baking tests, it was determined visually as the outer dried and darker zone of samples, which probably differs from the concept applied for simulation results. Actually, an accurate definition of the crust is not available, being subject of study currently (Vanin, Lucas & Trystram, 2009). Based on the presented results, the SHMT model was validated. Differences found between experimental and simulated profiles may be due to uncertainties in thermophysical properties of bread crust, such as water activity, mass diffusivity, and thermal conductivity, since is the zone where occur the most significant changes in temperature and water content during baking (Zhang & Datta, 2006). In addition, monitoring the dynamics in the crust during the process is a difficult task (Purlis & Salvadori, 2009b, Vanin et al., 2009).

From a general point of view, the proposed mathematical model properly describes a moving boundary problem with SHMT. Figure 8 shows typical local temperature and water content profiles (between centre and surface) obtained by simulation (note that the boundary is moving due to volume change), which are similar to the ones observed during other processes where the phase transition occurs in a moving interface, e.g. drying, frying, heating of materials with high moisture, freezing, thawing (Datta, 2007; Farid, 2002; Farid & Kizilel, 2009). In such situations, two different regions are well defined once the temperature of phase transition has been reached: a region with uniform values or smooth profiles of temperature and moisture, and a zone with marked profiles of these variables. In the case of bread baking, such regions are the crumb and the crust, respectively. Then, these zones are separated by the phase transition front: Figure 9 shows the position of evaporation front for an arbitrary simulated condition. A physical criterion to determine the position of the phase change moving front is to identify the zone where a sharp change occurs in temperature or water content of the product (Vanin et al., 2009). As can be seen in Figure 9, the proposed model is in agreement with this definition.

As was previously explained, the volume change occurring during the process was simulated through experimental data obtained in baking tests (Figure 10a). Note that the assumption of describing the volume change by the variation in the cross-section area is adequate since the axial expansion is negligible respect to change occurring in the cross-section (Sommier et al., 2005). It was not the objective of this work to explain the behaviour observed for different baking conditions regarding volume change, since the expansion and shrinkage of bread are very complex and specific phenomena. However, we can say that depending on heat and mass transfer fluxes, thermal expansion and structure stiffening will develop and interact in different ways leading to diverse volume change variations. For numerical solution of the model, the finite element mesh was deformed applying a Laplace smoothing, so the mesh velocity was described by Eq. (32). Figure 10b illustrates how a mesh consisting in seven nodes (for simplicity) is deformed with time, according to volume change observed in 220 ºC baking under forced convection. Solving Eq. (32), it can be stated that displacement of nodes is a linear function of spatial coordinate, so the displacement of nodes increases from the centre to surface (Figure 10b).

As a summary, Figure 11 shows the evolution of bread composition, in terms of crumb and crust, along baking. In other words, Figure 11 represents the objective of the present paper: it describes a moving boundary problem in a food material undergoing volume change. The proportion crumb/crust depends on simultaneous heat and mass transfer that determines the position and advancing of the evaporation front. At the same time, the volume of the product is changing according to specific mechanisms of expansion and shrinkage.

Finally, the influence of volume change on heat and mass transfer was studied by simulation of bread baking at 220 ºC under forced convection for three different conditions: (1) considering the actual volume change; (2) neglecting volume change (i.e. fixed mesh); (3) assuming a continuous shrinkage, which was measured in other condition as described in Section 4.2 (Figure 10a). Then, we focused on temperature profile of the core to do the analysis (Figure 12). The different patterns of volume change produced different temperature profiles due to the modification of temperature gradient. Considering the experimental profile as reference, the following predictions errors (Eq. (34)) were calculated for tested conditions: (1) 2.32% (SD = 2.19); (2) 4.04% (SD = 4.16); (3) 5.64% (SD = 5.67). In the studied case, differences could result negligible from a technological point of view, but it should be note that volume change certainly influences transport phenomena and the magnitude will depend on each particular process.

6. Conclusions

Several food processes can be represented by a moving boundary problem with simultaneous heat and mass transfer and volume change. In this work we developed a mathematical formulation to solve numerically this general problem and the proposed approach was successfully applied for simulation of bread baking. The general problem involves two aspects: transport phenomena and variable domain. The former was solved by a moving boundary formulation while the later through the Arbitrary Lagrangian-Eulerian method. The proposed approach gives the possibility of handling simple equations with continuous equivalent thermophysical properties, valid for the entire operating range, where no empirical parameters or imposed or fictitious boundary conditions are used to determine the position of the phase transition front. Though the volume change was included in an empirical way in this work, the formulation can be coupled with any other model describing expansion or shrinkage of material. For example, solid mechanics can be used to model volume change of bread during baking (this problem will be focus of future work).

Acknowledgments

Authors would like to thank to Eng. Sandro M. Goñi for helpful discussion when preparing the manuscript. This research was supported by grants from Consejo Nacional de Investigaciones Científicas y Técnicas (CONICET), Agencia Nacional de Promoción Científica y Tecnológica (ANPCyT, PICT 2007-01090), and Universidad Nacional de La Plata (UNLP) from Argentina.

Nomenclature

A	Cross-section area, m^2
a_w	Water activity
$\widetilde{C}$	Equivalent heat capacity, J m^{-3} K^{-1}
C	Heat capacity, J m^{-3} K^{-1}
C_p	Specific heat, J kg^{-1} K^{-1}
D	Water (liquid or vapour) diffusion coefficient of product, m^2 s^{-1}
D_{va}	Water vapour diffusion coefficient in air, m^2 s^{-1}
e_{abs}	Mean absolute percentage error, %
f	Surface temperature, K
H	Enthalpy, J m^{-3}
h	Heat transfer coefficient, W m^{-2} K^{-1}
k	Thermal conductivity, W m^{-1} K^{-1}
k_g	Mass transfer coefficient, kg Pa^{-1} m^{-2} s^{-1}
L	Characteristic length, m
P	Water vapour pressure, Pa
R, r	Radius, m
RH	Relative humidity, %
S	Interface position, m
SD	Standard deviation
T	Temperature, K
t	Time, s
u	Dependent variable, Eq. (33)
v_b	Boundary velocity, m s^{-1}

W	Water (liquid or vapour) content, kg kg^{-1}
X	Reference coordinate, m
x	Spatial coordinate, m
y	Input of delta function, Eq. (17)-(18)

Greek symbols

δ	Delta function
ΔT	Temperature range of phase change, K
ε	Emissivity
λ	Heat of phase change, J m^{-3}
λ_v	Latent heat of evaporation, J kg^{-1}
ρ	Density, kg m^{-3}
σ	Stefan-Boltzmann constant, 5.67×10^{-8} W m^{-2} K^{-4}
φ	Initial temperature distribution, K

Subscripts

0	Initial
1	Solid region
2	Liquid region
∞	Ambient
eq	Equivalent
f	Phase change
s	Solid or surface
sat	Saturated
w	Water

References

Białobrzewski, I. (2006). Simulation of changes in the density of an apple slab during drying. *International Communications in Heat and Mass Transfer, 33* (7), 880-888.

Białobrzewski, I., Zielińska, M., Mujumdar, A. S., & Markowski, M. (2008). Heat and mass transfer during drying of a bed of shrinking particles – Simulation for carrot cubes dried in a spout-fluidized-bed drier. *International Journal of Heat and Mass Transfer, 51* (19-20), 4704-4716.

Bonacina, C., Comini, G., Fasano, A., & Primicerio, M. (1973). Numerical solution of phase-change problems. *International Journal of Heat and Mass Transfer, 16* (10), 1825-1832.

Bouddour, A., Auriault, J.-L., Mhamdi-Alaoui, M., & Bloch, J. F. (1998). Heat and mass transfer in wet porous media in presence of evaporation-condensation. *International Journal of Heat and Mass Transfer, 41* (15), 2263-2277.

Bracewell, R. (2000). *The Fourier transform and its applications* (3rd ed.). New York: McGraw-Hill.

Campañone, L. A., Salvadori, V. O., & Mascheroni, R. H.(2001). Weight loss during freezing and storage of unpackaged foods. *Journal of Food Engineering, 47* (2), 69-79.

COMSOL AB (2005). *COMSOL Multiphysics Modeling Guide*. Sweden: COMSOL AB.

Crank, J. (1987). *Free and moving boundary problems*. UK: Oxford University Press.

Datta, A. K. (2007). Porous media approaches to studying simultaneous heat and mass transfer in food processes. II: Property data and representative results. *Journal of Food Engineering, 80* (1), 96-110.

de Vries, U., Sluimer, P., & Bloksma, A. H. (1989). A quantitative model for heat transport in dough and crumb during baking. In N. G. Asp, *Cereal Science and Technology in Sweden*, (pp. 174-188). Sweden: Lund University Chemical Centre.

Donea, J., Huerta, A., Ponthot, J.-Ph., & Rodríguez-Ferran, A. (2004). Arbitrary Lagrangian-Eulerian methods. In E. Stein, R. de Borst & T. J. R. Hughes, *Encyclopedia of Computational Mechanics, Volume 1: Fundamentals*, (Chapter 14). UK: John Wiley & Sons, Ltd.

Duarte, F., Gormaz, R., & Natesan, S. (2004). Arbitrary Lagrangian-Eulerian method for Navier-Stokes equations with moving boundaries. *Computer Methods in Applied Mechanics and Engineering, 193* (45-47), 4819-4836.

Farid, M. (2002). The moving boundary problems from melting and freezing to drying and frying of food. *Chemical Engineering and Processing, 41* (1), 1-10.

Farid, M., & Kizilel, R. (2009). A new approach to the analysis of heat and mass transfer in drying and frying of food products. *Chemical Engineering and Processing: Process Intensification, 49* (1), 217-223.

Fletcher, C. A. J. (1991). *Computational techniques for fluid dynamics 1: Fundamentals and general techniques* (2nd ed.). Germany: Springer-Verlag.

Hamdami, N., Monteau, J.-Y., & Le Bail, A. (2004). Heat and mass transfer in par-baked bread during freezing. *Food Research International, 37* (5), 477-488.

Heizer, J., & Render, B. (2004). *Principles of operations management* (5th ed.). New Jersey: Prentice Hall.

Lostie, M., Peczalski, R., Andrieu, J., & Laurent, M. (2002). Study of sponge cake batter baking process. Part I: experimental data. *Journal of Food Engineering, 51* (2), 131-137.

Luikov, A. V. (1975). Systems of differential equations of heat and mass transfer in capillary-porous bodies (review). *International Journal of Heat and Mass Transfer, 18* (1), 1-14.

Mascarenhas, W. J., Akay, H. U., & Pikal, M. J. (1997). A computational model for finite element analysis of the freeze-drying process. *Computer Methods in Applied Mechanics and Engineering, 148* (1-2), 105-124.

Mayor, L., & Sereno, A. M. (2004). Modelling shrinkage during convective drying of food materials: A review. *Journal of Food Engineering, 61* (3), 373-386.

Mondal, A., & Datta, A. K. (2008). Bread baking – A review. *Journal of Food Engineering, 86* (4), 465-474.

Olguín, M. C., Salvadori, V. O., Mascheroni, R. H., & Tarzia, D. A. (2008). An analytical solution for the coupled heat and mass transfer during the freezing of high-water content materials. *International Journal of Heat and Mass Transfer, 51* (17-18), 4379-4391.

Purlis, E. (2007). *Simulación de las transferencias simultáneas de materia y energía en el proceso de horneado de pan mediante elementos finitos*. PhD thesis, Universidad Nacional de Quilmes, Argentina.

Purlis, E., & Salvadori, V.O. (2009a). Bread baking as a moving boundary problem. Part 1: Mathematical modelling. *Journal of Food Engineering*, *91* (3), 428-433.

Purlis, E., & Salvadori, V.O. (2009b). Bread baking as a moving boundary problem. Part 2: Model validation and numerical simulation. *Journal of Food Engineering*, *91* (3), 434-442.

Scanlon, M. G., & Zghal, M. C. (2001). Bread properties and crumb structure. *Food Research International, 34* (10), 841-864.

Sluimer, P., & Krist-Spit, C. E. (1987). Heat transport in dough during the baking of bread. In I. D. Morton, *Cereals in a European Context*, (pp. 355-363). Chicester, UK: Ellis Horwood Ltd.

Sommier, A., Chiron, H., Colonna, P., Della Valle, G., & Rouillé, J. (2005). An instrumented pilot scale oven for the study of French bread baking. *Journal of Food Engineering, 69* (1), 97-106.

Vanin, F. M., Lucas, T., & Trystram, G. (2009). Crust formation and its role during bread baking. *Trends in Food Science & Technology, 20* (8), 333-343.

Wagner, M. J., Lucas, T., Le Ray, D., & Trystram, G. (2007). Water transport in bread during baking. *Journal of Food Engineering, 78* (4), 1167-1173.

Welty, J. R., Wicks, C. E., & Wilson, R. E. (1976). *Fundamentals of momentum, heat, and mass transfer* (2nd ed.). New York: John Wiley & Sons.

Zanoni, B., Peri, C., & Pierucci, S. (1993). A study of the bread-baking process. I: A phenomenological model. *Journal of Food Engineering, 19* (4), 389-398.

Zanoni, B., Pierucci, S., & Peri, C. (1994). Study of the bread baking process – II. Mathematical modelling. *Journal of Food Engineering, 23* (3), 321-336.

Zhang, J., & Datta, A. K. (2004). Some considerations in modeling of moisture transport in heating of hygroscopic materials. *Drying Technology, 22* (8), 1983-2008.

Zhang, J., & Datta, A. K. (2006). Mathematical modeling of bread baking process. *Journal of Food Engineering, 75* (1), 78-89.

Zienkiewicz, O. C. (1989). *The finite element method*. New York: McGraw-Hill.

Figure captions

Figure 1. (a) Smoothed Heaviside function (in blue) used to incorporate the phase transition into thermophysical properties according to description in Section 2.2. In Eq. (17) and (18), $y = T - T_f$ and $\Delta y = \Delta T$, with $T_f = 100$ ºC and $\Delta T = 0.5$ ºC. The delta-type function $\delta(T - T_f, \Delta T)$ is used to describe the enthalpy jump (in red). (b) Typical variation of thermal conductivity (k, in blue) and specific heat (C_p, in red) of bread during baking (obtained from simulation at 200 ºC under forced convection).

Figure 2. Block diagram of the numerical solution procedure described in Section 3. PDE: partial differential equations; BC: boundary conditions; SHMT: simultaneous heat and mass transfer; FEM: finite element method; DAE: differential algebraic equations; ALE: arbitrary Lagrangian-Eulerian.

Figure 3. Sampling regions for determination of water content distribution in bread during baking. The schema represents the central cross-section (1 cm thickness) in the axial direction of bread.

Figure 4. Measurement of cross-section area of bread by image processing. (a) Original RGB image of a sample (front view). (b) Binary image obtained by segmentation after grey-scale transformation, intensity adjustment and filtering stages.

Figure 5. Experimental (symbols) and simulated (lines) temperature profiles at different zones of bread, i.e. core (squares), intermediate (circles) and surface (triangles), during

baking at 200 °C under (a) natural convection and (b) forced convection. Experimental values every 1 min are shown for simplicity.

Figure 6. Experimental (symbols) and simulated (lines) temperature profiles at different zones of bread, i.e. core (squares), intermediate (circles) and surface (triangles), during baking at 220 °C under (a) natural convection and (b) forced convection. Experimental values every 1 min are shown for simplicity.

Figure 7. (a) Water content and (b) crust thickness of bread during baking at 220 ºC under natural convection. In (a): squares and dash line account for crumb, and triangles and continuous line correspond to crust. Symbols and lines represent experimental and simulated data, respectively.

Figure 8. Simulated (a) temperature and (b) water content profiles during baking at 220 ºC under natural convection for different times (min): 7 (black), 14 (blue), 21 (green), and 28 (red).

Figure 9. Simulated temperature and water content profiles corresponding to 28 min baking at 220 ºC under natural convection. Evaporation front position is calculated according to Zhang and Datta (2004).

Figure 10. (a) Relative equivalent radius, i.e. $R_{eq}(t)/R_{eq}(t = 0)$, of bread during baking. Triangles represent 200 ºC and circles represent 220 ºC oven temperature. Filled symbols show natural convection and empty symbols show forced convection condition. Squares account for 180 ºC baking under forced convection. (b) Deformation

with time of a seven-node mesh according to volume change observed during baking at 220 ºC under forced convection.

Figure 11. Variation of bread boundary and evaporation front positions during baking at 220 ºC under forced convection obtained from simulation.

Figure 12. Core temperature profiles at bread during baking at 220 ºC under forced convection. Lines correspond to different simulated conditions for volume change: thick line for actual volume change, normal line for fixed mesh, and dashed line for continuous shrinkage. Circles represent experimental data.

ACCEPTED MANUSCRIPT

Figure 1 – Purlis and Salvadori

(a)

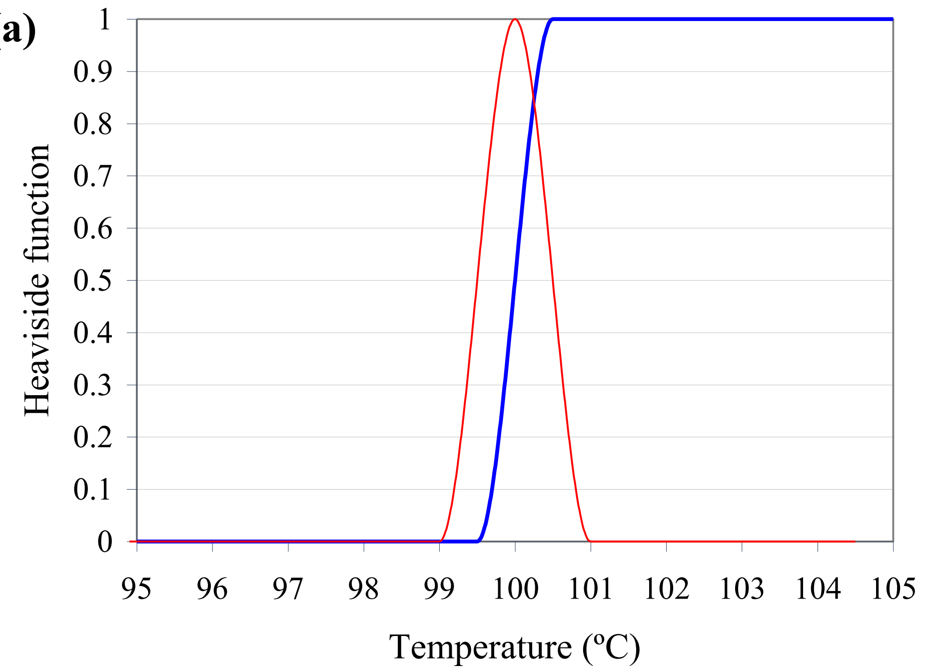

(b)

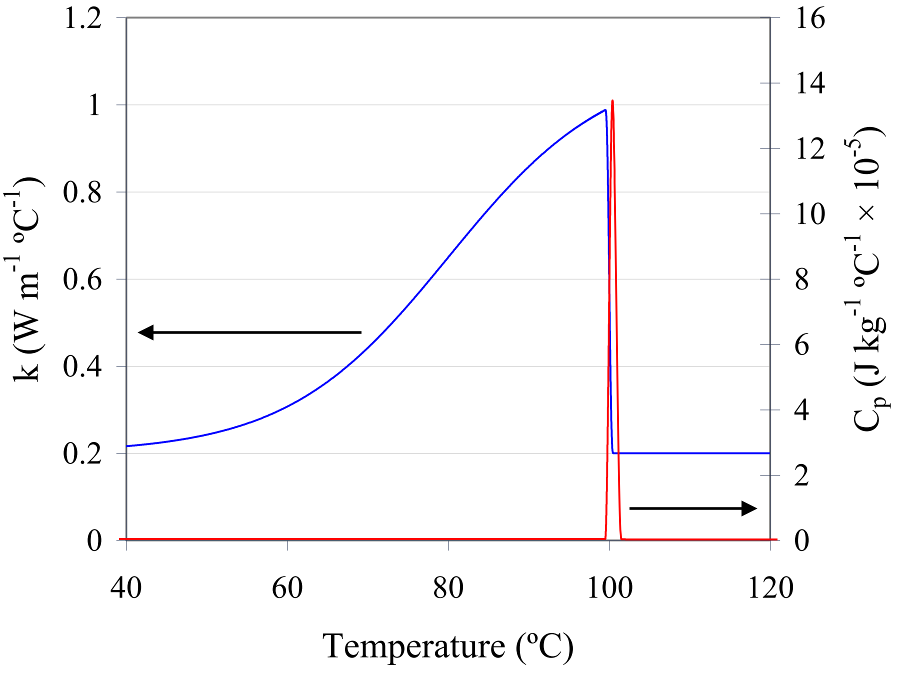

Figure 2 – Purlis and Salvadori

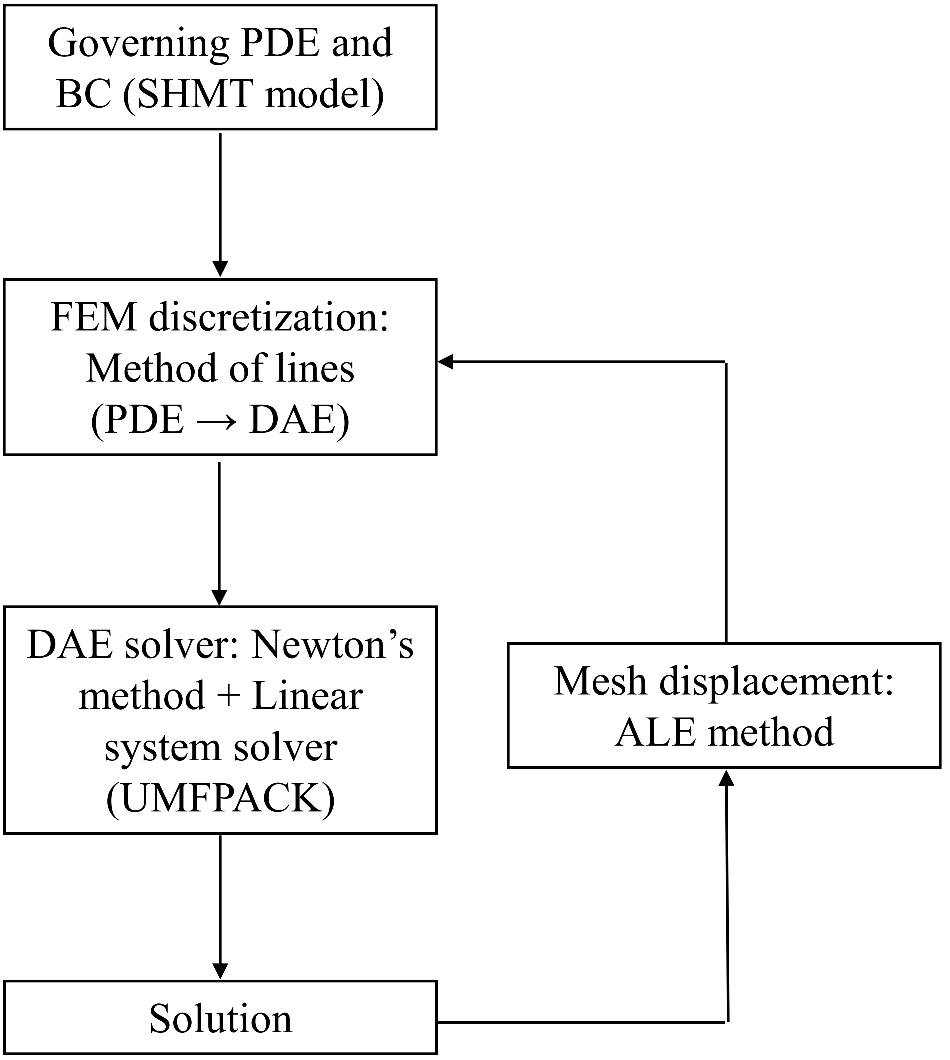

Figure 3 – Purlis and Salvadori

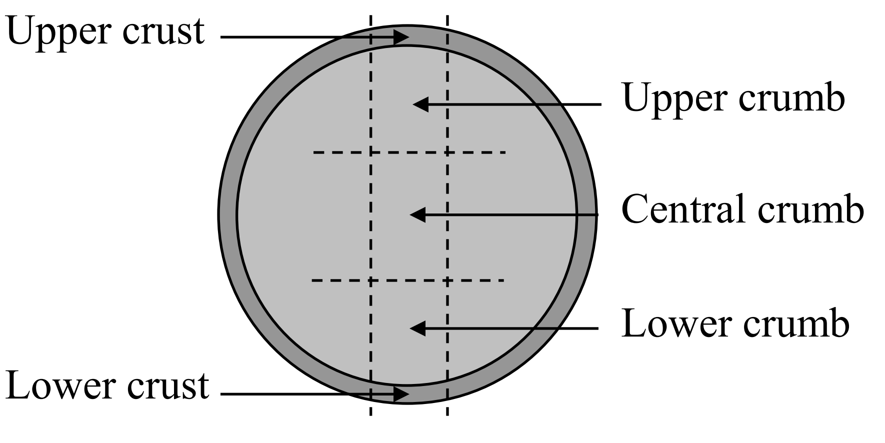

Figure 4 – Purlis and Salvadori

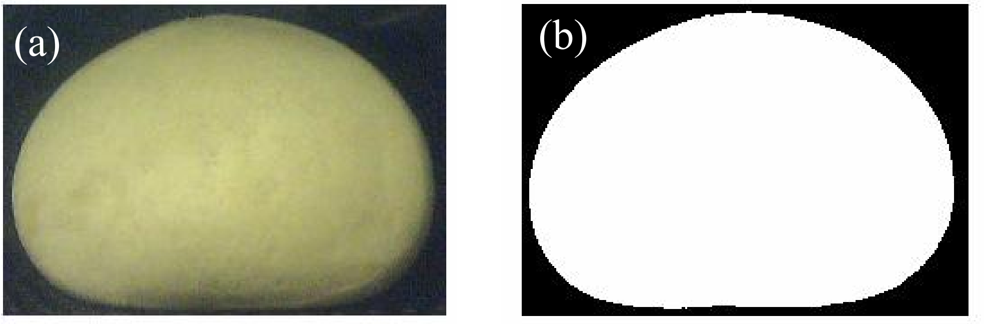

Figure 5 – Purlis and Salvadori

(a)

(b)

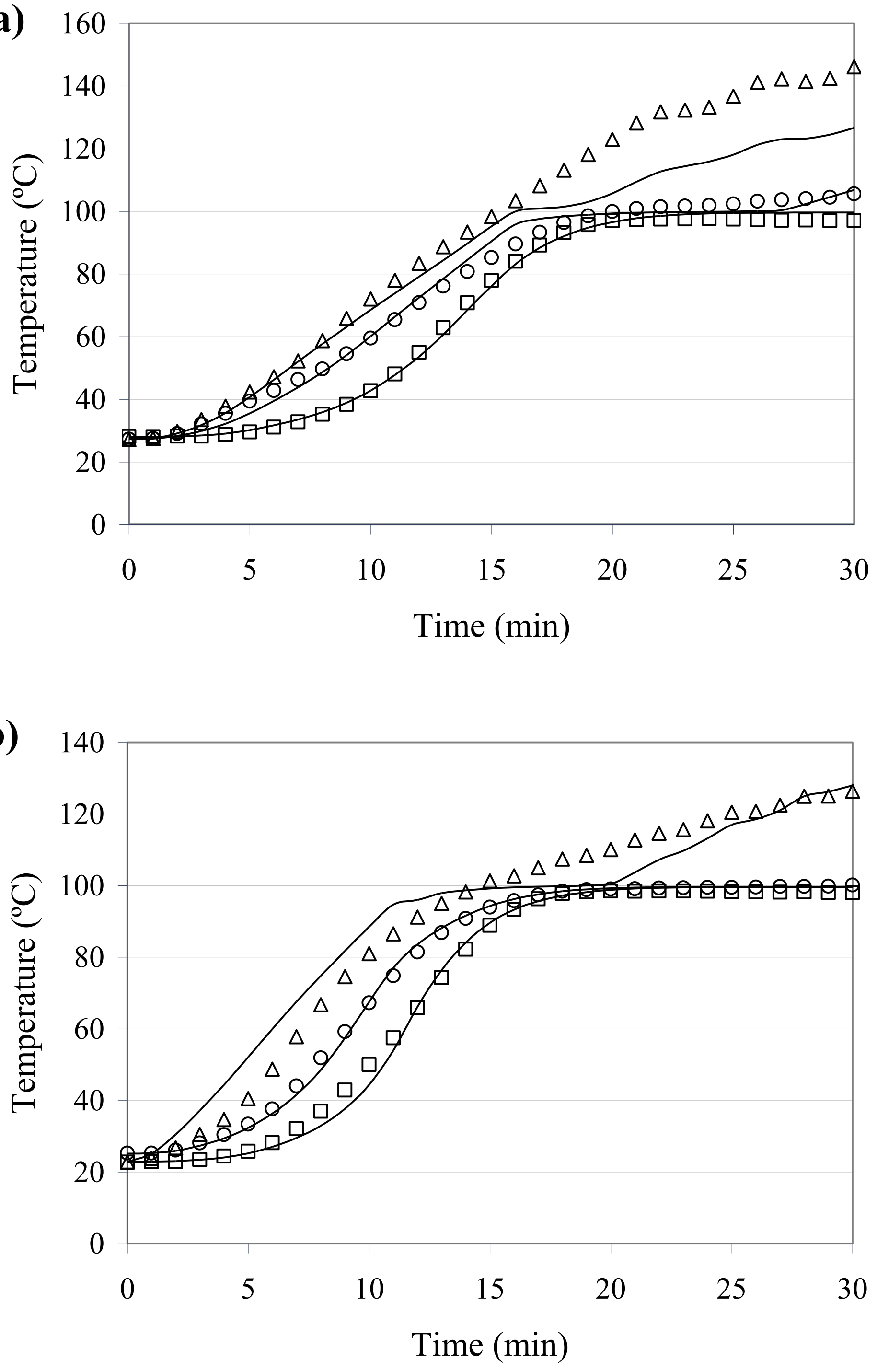

Figure 6 – Purlis and Salvadori

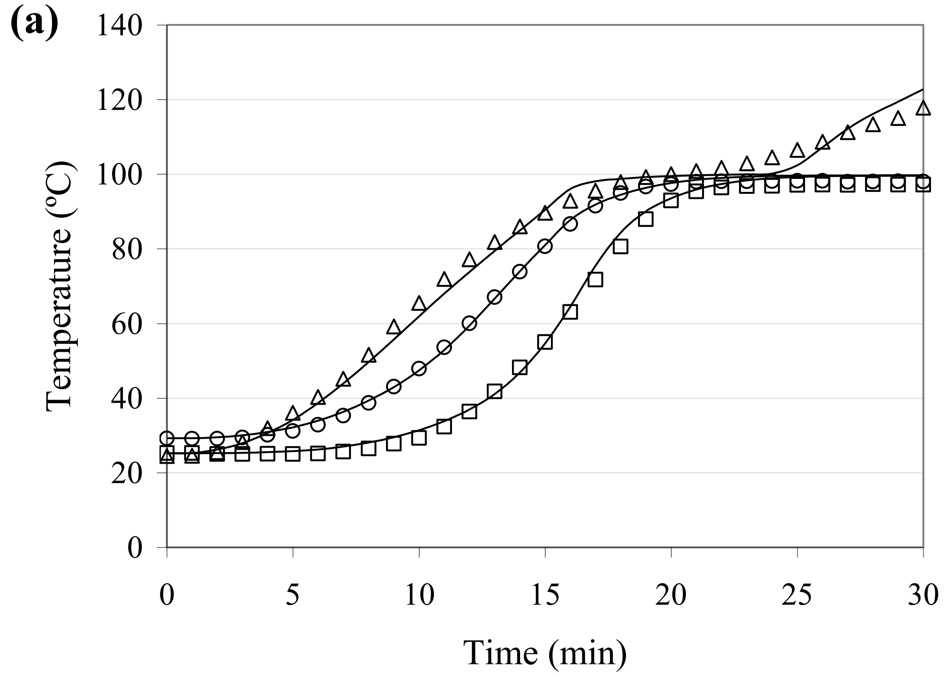

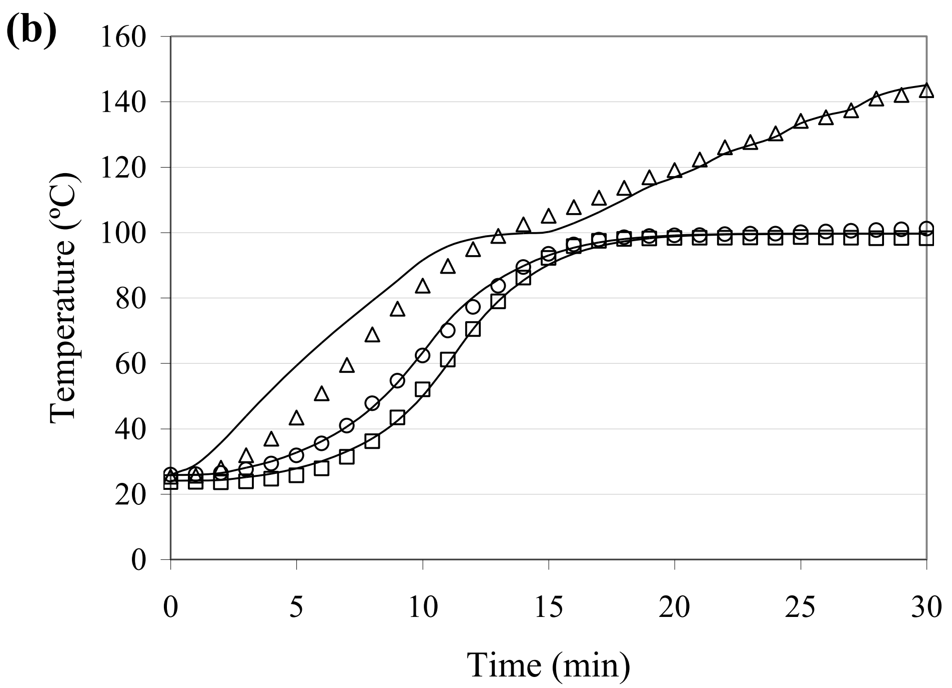

Figure 7 – Purlis and Salvadori

(a)

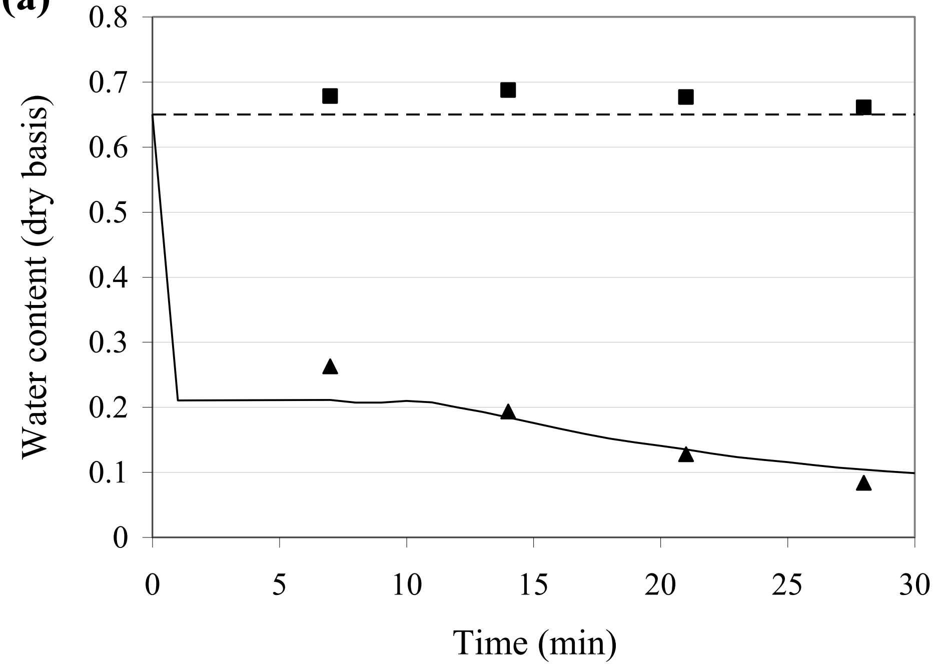

(b)

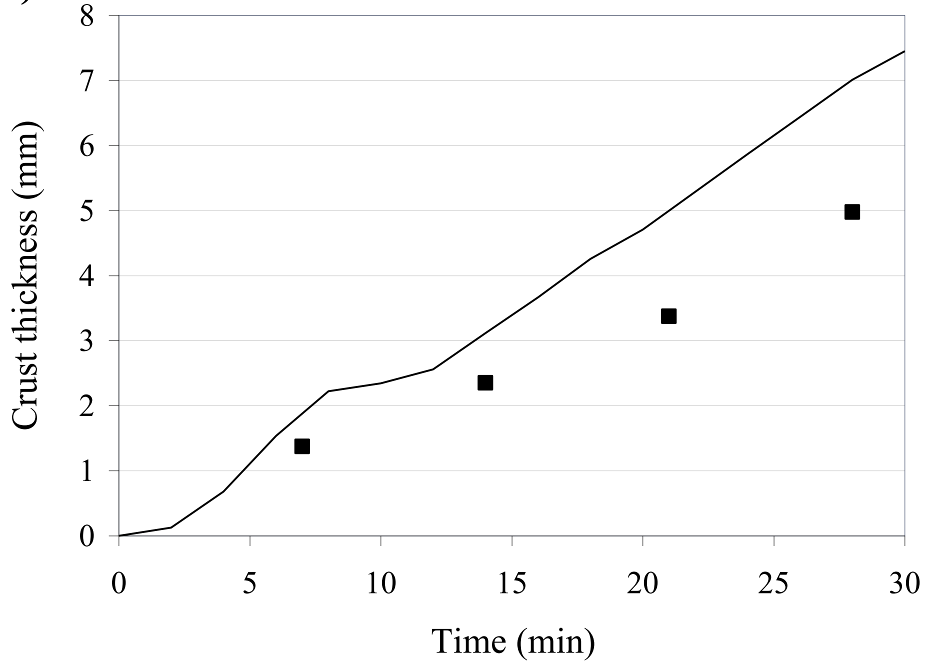

Figure 8 – Purlis and Salvadori

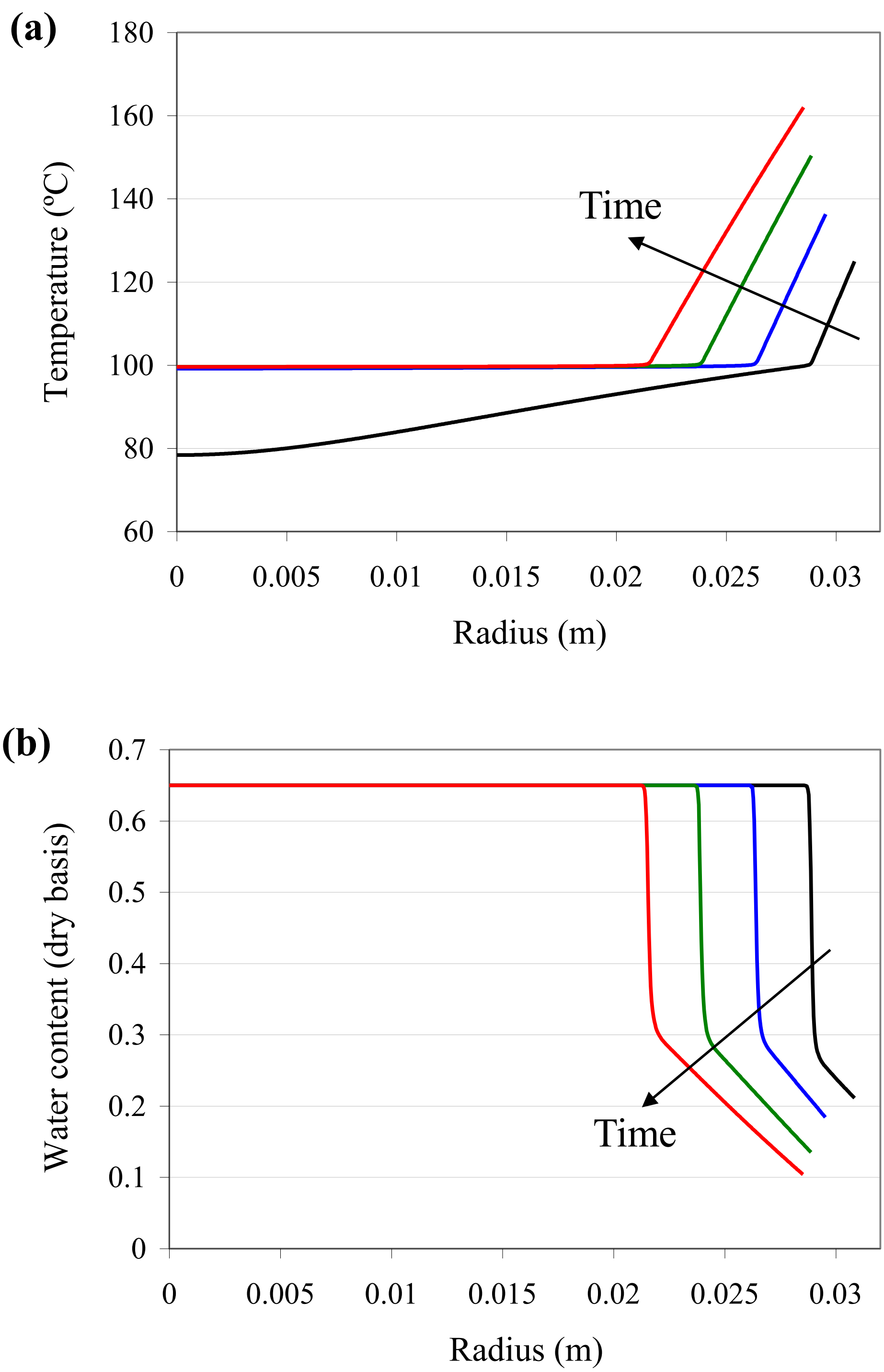

Figure 9 – Purlis and Salvadori

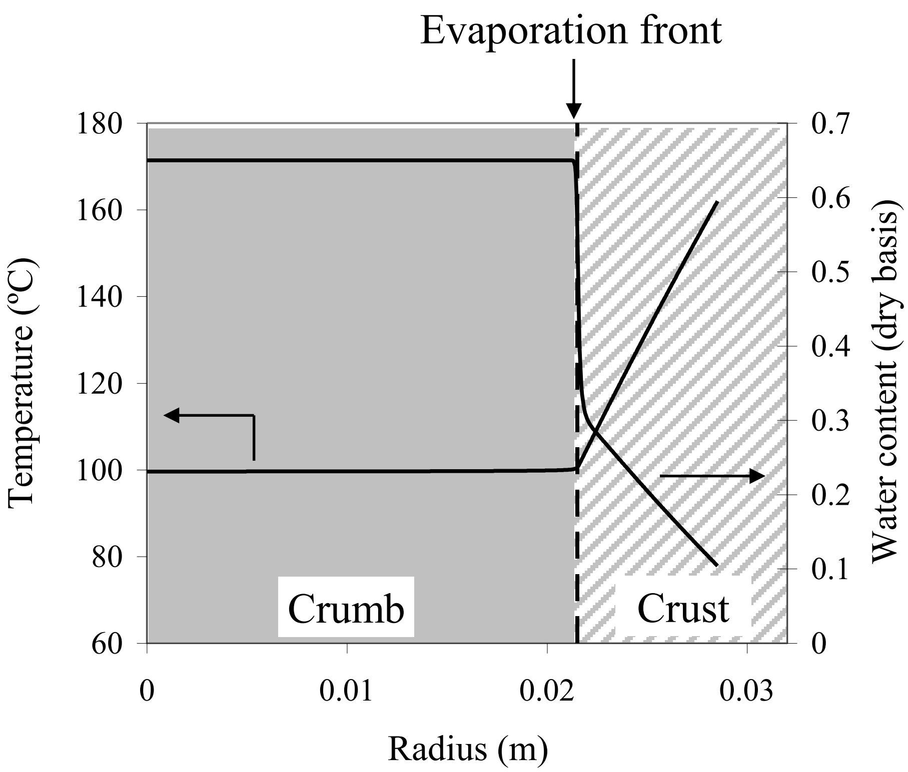

Figure 10 – Purlis and Salvadori

(a)

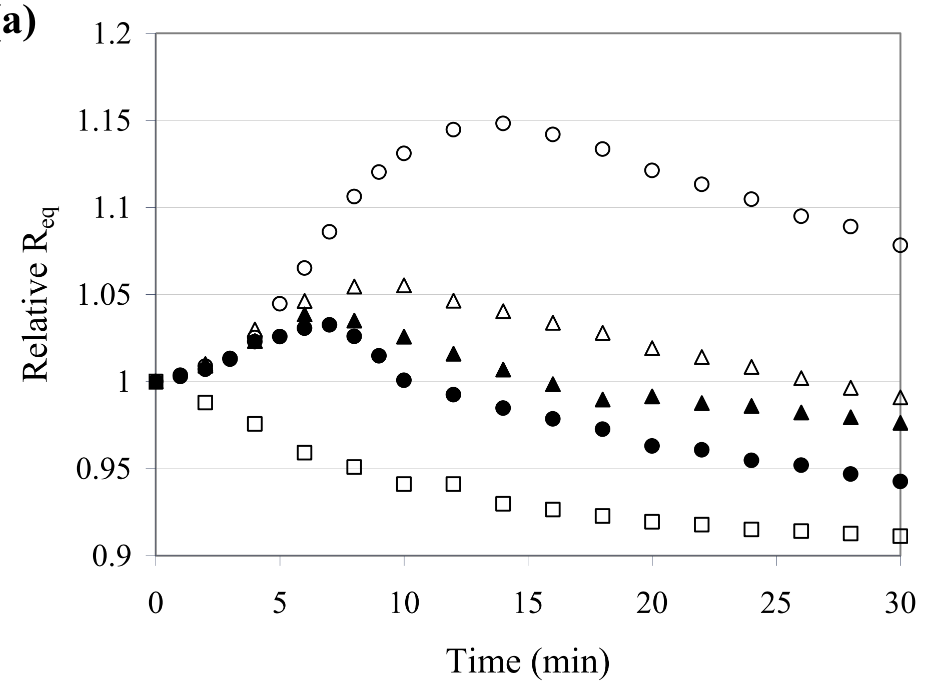

(b)

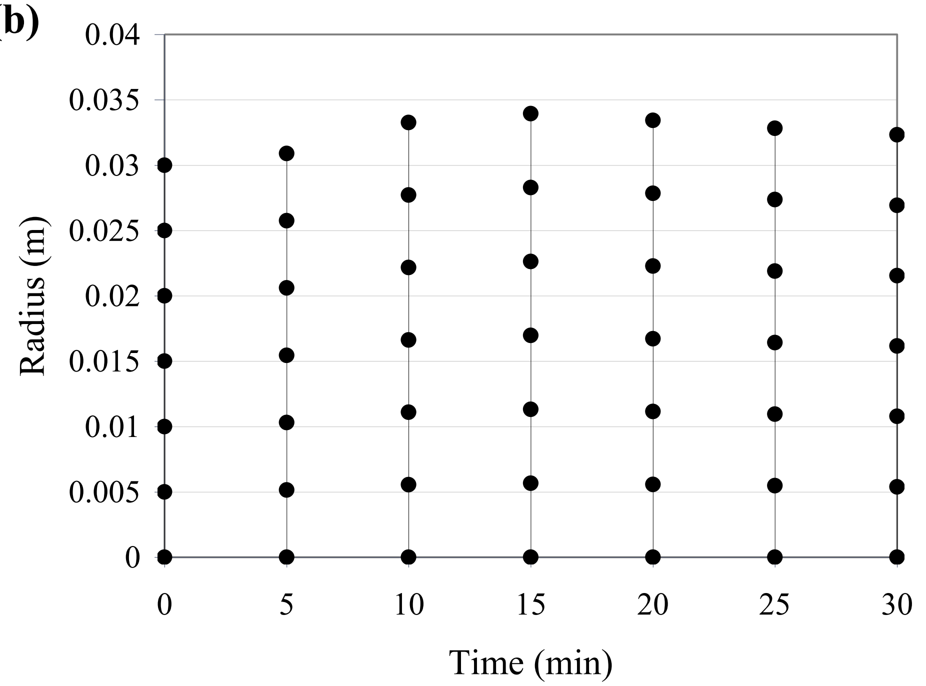

Figure 11 – Purlis and Salvadori

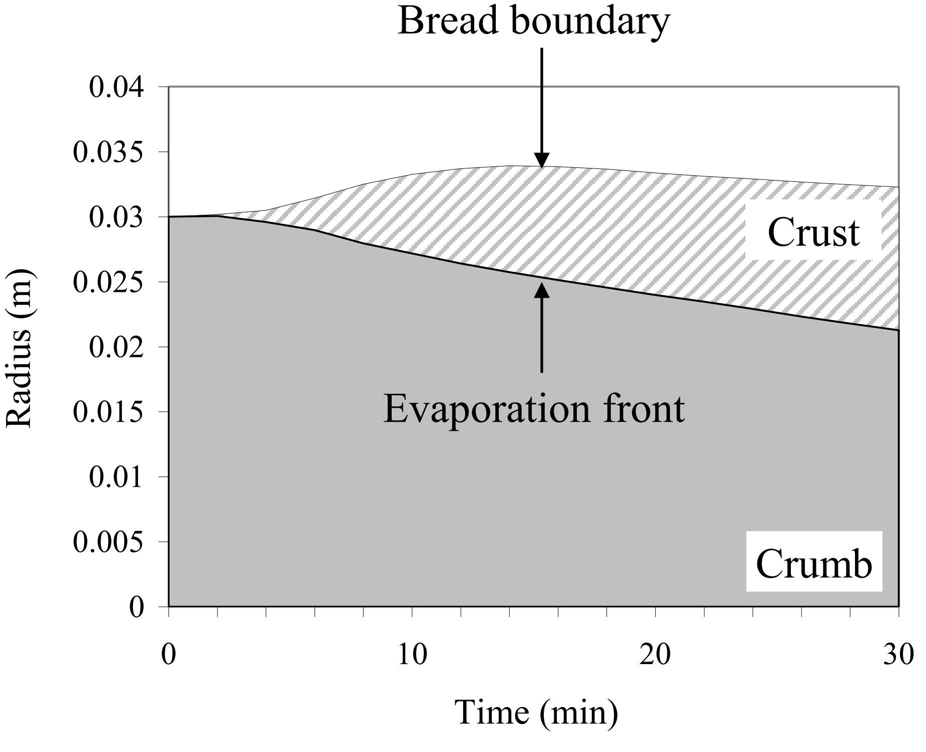

Figure 12 – Purlis and Salvadori

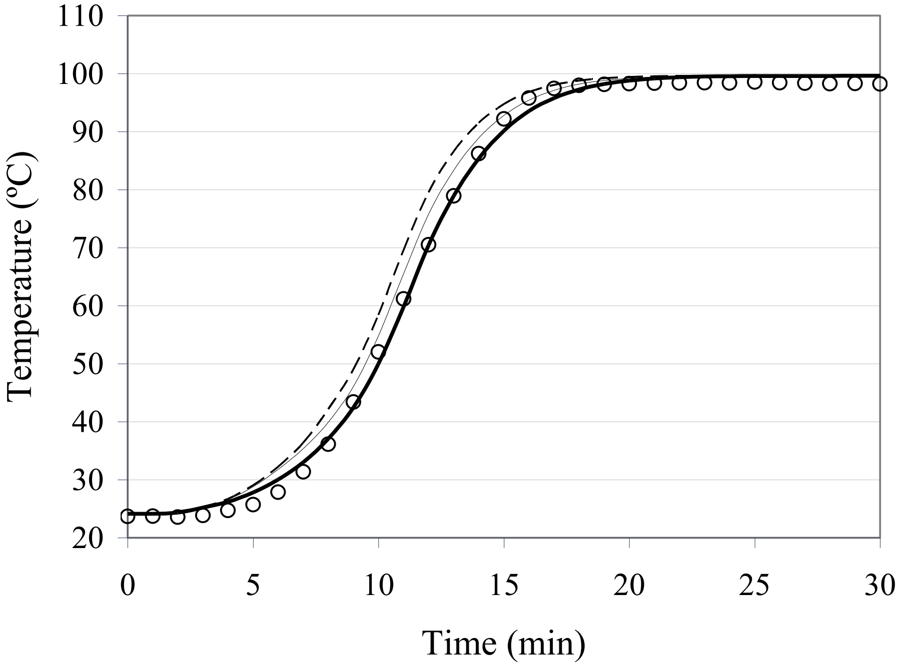

Table 1

Values for heat (h, in W m^{-2} K^{-1}) and mass (k_g, in kg Pa^{-1} m^{-2} s^{-1}) transfer coefficients (Purlis & Salvadori, 2009b).

Baking temperature (ºC)	Natural convection		Forced convection	
	h	k_g	h	k_g
200	7.68	3.38×10^{-9}	11.96	8.46×10^{-9}
220	7.95	6.04×10^{-9}	11.97	8.46×10^{-9}

Table 2

Mean absolute percentage error (e_{abs}, Eq. (34)) for temperature prediction (profiles shown in Figures 5 and 6). For a 30 min process, n = 360 since sampling time was 5 sec. Standard deviation is shown in parentheses. NC: natural convection; FC: forced convection.

Location	200 ºC, NC	220 ºC, NC	200 ºC, FC	220 ºC, FC
Core	1.53 (0.91)	2.67 (1.87)	2.59 (3.45)	2.32 (2.19)
Intermediate	3.18 (2.66)	1.30 (0.94)	1.37 (1.70)	1.16 (1.11)
Surface	7.61 (5.03)	2.85 (1.63)	8.37 (7.80)	9.53 (12.38)

Table 3

Experimental (EXP) and simulated (SIM) water content (dry basis) and thickness of bread crust during baking. Standard deviation is shown in parentheses. NC: natural convection; FC: forced convection.

		Water content (kg kg^{-1})		Crust thickness (mm)	
Condition	Time (min)	EXP	SIM	EXP	SIM
200 ºC, NC	10	0.24 (0.02)	0.26	1.3 (0.1)	2.1
	20	0.13 (0.01)	0.23	2.8 (0.4)	4.0
	30	0.09 (0)	0.16	4.0 (0.4)	6.5
220 ºC, NC	7	0.26 (0.06)	0.21	1.4 (0.3)	1.9
	14	0.19 (0.03)	0.18	2.4 (0.5)	3.1
	21	0.13 (0)	0.14	3.4 (0.8)	5.0
	28	0.08 (0.03)	0.10	5.0 (0.8)	7.0
200 ºC, FC	10	0.23 (0)	0.15	1.8 (0.1)	3.4
	20	0.14 (0.03)	0.11	3.4 (0.2)	5.6
	30	0.10 (0)	0.09	4.1 (0.1)	7.6
220 ºC, FC	7	0.23 (0.05)	0.14	1.6 (0.4)	3.5
	14	0.16 (0.03)	0.08	2.6 (0.3)	8.2
	21	0.12 (0)	0.07	3.6 (0.5)	9.6
	28	0.09 (0.01)	0.06	4.7 (0.6)	10.7